EBioMedicine 2 (2015) 456–466

Contents lists available at ScienceDirect

EBioMedicine

journal homepage: www.ebiomedicine.com

Original Article

Mitochondrial-dependent Autoimmunity in Membranous Nephropathy of IgG4-related Disease

Simona Buelli [a,1], Luca Perico [a,1], Miriam Galbusera [a], Mauro Abbate [a], Marina Morigi [a], Rubina Novelli [a], Elena Gagliardini [a], Chiara Tentori [a], Daniela Rottoli [a], Ettore Sabadini [b], Takao Saito [c], Mitsuhiro Kawano [d], Takako Saeki [e], Carlamaria Zoja [a], Giuseppe Remuzzi [a,b,1,*], Ariela Benigni [a,1]

[a] IRCCS — Istituto di Ricerche Farmacologiche "Mario Negri", Centro Anna Maria Astori, Science and Technology Park Kilometro Rosso, Bergamo, Italy
[b] Unit of Nephrology and Dialysis, Azienda Ospedaliera Papa Giovanni XXIII, Bergamo, Italy
[c] General Medical Research Center, Faculty of Medicine, Fukuoka University, Japan
[d] Department of Rheumatology, University School of Medicine, Kanazawa, Japan
[e] Department of Internal Medicine, Red Cross Hospital, Nagaoka, Japan

ARTICLE INFO

Article history:
Received 3 December 2014
Received in revised form 4 March 2015
Accepted 5 March 2015
Available online 7 March 2015

Keywords:
IgG4-related disease
Membranous nephropathy
Carbonic anhydrase II
Superoxide dismutase 2
Podocyte

ABSTRACT

The pathophysiology of glomerular lesions of membranous nephropathy (MN), including seldom-reported IgG4-related disease, is still elusive. Unlike in idiopathic MN where IgG4 prevails, in this patient IgG3 was predominant in glomerular deposits in the absence of circulating anti-phospholipase A_2 receptor antibodies, suggesting a distinct pathologic process. Here we documented that IgG4 retrieved from the serum of our propositus reacted against carbonic anhydrase II (CAII) at the podocyte surface. In patient's biopsy, glomerular CAII staining increased and co-localized with subepithelial IgG4 deposits along the capillary walls. Patient's IgG4 caused a drop in cell pH followed by mitochondrial dysfunction, excessive ROS production and cytoskeletal reorganization in cultured podocytes. These events promoted mitochondrial superoxide-dismutase-2 (SOD2) externalization on the plasma membrane, becoming recognizable by complement-binding IgG3 anti-SOD2. Among patients with IgG4-related disease only sera of those with IgG4 anti-CAII antibodies caused low intracellular pH and mitochondrial alterations underlying SOD2 externalization. Circulating IgG4 anti-CAII can cause podocyte injury through processes of intracellular acidification, mitochondrial oxidative stress and neoantigen induction in patients with IgG4 related disease. The onset of MN in a subset of patients could be due to IgG4 antibodies recognizing CAII with consequent exposure of mitochondrial neoantigen in the context of multifactorial pathogenesis of disease.

1. Introduction

Hyper-IgG4-associated abnormalities are common denominators for several autoimmune fibroinflammatory diseases that can affect any organ from the salivary glands to the pancreas or kidneys, collectively referred to as IgG4-related disease [1]. Characteristic pathological features in various affected sites consist of lymphoplasmacytic infiltration with IgG4-positive plasma cells, storiform fibrosis, and variably elevated levels of IgG4 [1]. Kidney lesions are usually accompanied by tubulointerstitial nephritis [2]. Glomerular lesions, including membranous nephropathy (MN), have been reported less frequently [2,3].

We described a 54-year-old male patient with IgG4-related disease manifesting as pancreatitis, Mikulicz disease that later developed nephrotic-range proteinuria, and MN [4] with glomerular lesions partly different from the idiopathic form. Indeed the predominant immunoglobulin deposited in the renal tissue was IgG3, while staining for IgG4 was weak in the absence of circulating anti-phospholipase A_2 receptor (PLA_2R) antibodies, possibly implying a distinct process. Moreover, no detectable immune complexes were found in the patient's serum [4]. On the other hand, we found IgG3 reactivity against superoxide-dismutase-2 (SOD2) [4], a mitochondrial antioxidant previously identified as an autoimmune target in patients with idiopathic MN [5]. The first aim of this study was to clarify the role of IgG4 antibodies in our patient's renal disease, and cellular mechanisms underlying SOD2 enrichment on the podocyte plasma membrane. We also wanted to establish whether IgG4-related disease and MN development have a common pathogenic event. Addressing those questions in our patient and in four other IgG4-related disease patients without MN, allowed us to recapitulate the

* Corresponding author at: IRCCS — Istituto di Ricerche Farmacologiche "Mario Negri", Centro Anna Maria Astori, Science and Technology Park Kilometro Rosso, Via Stezzano, 87, 24126 Bergamo, Italy.
E-mail address: giuseppe.remuzzi@marionegri.it (G. Remuzzi).
[1] Contributed equally.

http://dx.doi.org/10.1016/j.ebiom.2015.03.003

pathogenetic chain of events taking advantage of *in vitro* disease modeling. Here we propose a two-stage model in which IgG4 anti-carbonic anhydrase II (CAII), an autoantigen candidate in IgG4-related disease patients, is critical for altering pH homeostasis, mitochondrial dynamic, and SOD2 corticalization. At a later stage, mislocated SOD2 serves as a target for the binding of IgG3-subtype autoantibodies capable of fixing complement and amplifying podocyte injury, which contribute to the MN lesion, likely favored by individual genetic predisposition.

2. Methods

2.1. Study Participants

We analyzed our propositus diagnosed with IgG4-related disease with autoimmune pancreatitis and Mikulicz disease admitted to the Nephrology Unit of the Ospedali Riuniti, Bergamo, Italy as reported [4]. Moreover, we enrolled four additional patients with a diagnosis of IgG4-related disease. Sera from patients with IgG4-related disease with tubulointerstitial nephritis (TIN) (IgG4-RD1, IgG4-RD2 and IgG4-RD4) or without renal involvement (IgG4-RD3) were provided by Professor Takao Saito (General Medical Research Center, Faculty of Medicine, Fukuoka University, Japan). The research protocols were approved by the Ethical Committee of the Clinical Research Center of the Mario Negri Institute, the Clinical Study Review Board at Fukuoka University Hospital and the Medical Ethics Committee of Kanazawa University. Written informed consent was obtained from each patient in accordance with the Declaration of Helsinki guidelines.

2.2. Total IgG and IgG4 Purification

IgG purification was performed through affinity chromatography using Affi-Prep-Protein A (Bio-Rad Laboratories, Hercules, CA) [6]. Serum was centrifuged (11,000 ×*g*, 20 min) and particulate and lipid fractions were removed. The sample diluted with binding buffer (glycine 1.5 M–NaCl 3 M, pH 8.9) was loaded on the column and eluted with citric acid 0.1 M, pH 3. The eluate was concentrated and dialyzed against PBS (phosphate 10 mM–NaCl 150 mM, pH 7.3) with Amicon concentrators (Amicon Ultra-15 100 KD, Millipore, Temecula, CA). IgG4 purification was performed using affinity chromatography with CaptureSelect IgG4 (Hu) affinity matrix (Life Technologies, Carlsbad, CA) containing a 12 kDa Llama antibody fragment recognizing human IgG4. The serum was applied to the column and eluted with glycine 0.1 M, pH 3. Sample was concentrated and dialyzed against PBS with Amicon concentrators. To prevent damage to immunoglobulins due to exposure to the acidic medium, for both total IgG and IgG4 purification, during the elution step the pH was continuously adjusted to neutrality by adding 1 M Tris pH 9 to the collecting tube.

2.3. Cell Culture and Incubations

Conditionally immortalized human podocytes (kindly provided by Prof. M.A. Saleem, Children's Renal Unit and Academic Renal Unit, University of Bristol, Southmead Hospital, Bristol) were differentiated for 12 days as previously described [7]. In preliminary experiments, we found that the patient's serum at the dilution of 1:3 had no cytotoxic effect (data not shown). Podocytes were incubated for different time intervals with RPMI 1640 medium (medium), H_2O_2 (150 μM), patient's serum (1:3), total IgG (1 mg/ml) or purified IgG4 (100 μg/ml) from the patient or from healthy volunteers (n = 3). To document the effect of the binding of anti-CAII IgG4 on SOD2 expression, podocytes were exposed for 15 h to anti-CAII antibody (5 μg/ml, Sigma-Aldrich) or to normal IgG (5 μg/ml, Santa Cruz Biotechnology, Santa Cruz, CA). In additional experiments, podocytes were exposed for 15 h to the patient's serum (1:3) that was pre-incubated with purified CAII (100 μg/ml for 6 h at 4 °C) to saturate the binding of IgG4 anti-CAII. To study the role of reactive oxygen species in F-actin remodeling, the SOD2 mimetic manganese (III) tetrakis (4-benzoic acid) porphyrin (mnTBAP) (100 μM, Santa Cruz Biotechnology) was used. The effect of the carbonic anhydrase II inhibitor acetazolamide (500 μM) on intracellular pH was also investigated. In selected experiments, sera (1:3) from other patients with IgG4-related disease were used.

2.4. Immunofluorescence Analysis on Cultured Podocytes

Differentiated podocytes were fixed in 2% paraformaldehyde (Electron Microscopy Science, Hatfield, PA) and 4% sucrose (Sigma-Aldrich, Milan, Italy) and nonspecific binding sites were blocked with 2% FBS, 2% bovine serum albumin and 0.2% bovine gelatin in PBS 1×. Cells were incubated with rabbit polyclonal anti-SOD2 antibody (1:500, Millipore, Eschborn, Germany) or anti-CAII antibody (1:10,000, Abcam) followed by incubation with the appropriate Cy3-conjugated secondary antibody (Jackson ImmunoResearch Laboratories, West Grove, PA). For colocalization analysis, cells were then incubated with a FITC-conjugated anti-human IgG3 (1:25, Sigma-Aldrich) or with a FITC-conjugated anti-C3 (1:25, Dako A/S, Glostrup, Denmark). CAII expression was evaluated with a rabbit polyclonal anti-CAII antibody (1:200, Abcam, Cambridge, UK) followed by a goat anti-rabbit Cy3-conjugated secondary antibody (Jackson ImmunoResearch Laboratories). To study F-actin rearrangement, fixed podocytes were permeabilized with 0.3% Triton X-100 (Sigma-Aldrich) and then incubated with rhodamine-phalloidin (20 U/ml, Molecular Probes Inc., Eugene, OR). Nuclei were counterstained with DAPI (Sigma-Aldrich). Negative controls were obtained by omitting primary antibodies. Samples were examined using a confocal inverted laser microscope (LSM 510 Meta; Zeiss, Jena, Germany). The quantification of externalized SOD2 on the plasma membrane and the count of podocytes with peripheral F-actin distribution were performed on 15 random fields per sample. Specifically, the area corresponding to the SOD2 staining was measured in pixels by using the Image J 1.40 g software and normalized for the number of nuclei identified by DAPI staining.

2.5. Podocyte Subcellular Fraction and Whole Extract Preparation

The subcellular fractionation of human podocytes was performed as previously described [8] with minor modifications. After incubations, cells were gently scraped and incubated in hypotonic lysis buffer (10 mM Tris–HCl pH 7.4, 2 mM EDTA, 200 μM PMSF, 1 mM benzamidine, 10 μg/ml pepstatin and 10 μg/ml leupeptin) for 20 min on ice and then lysed by sonication. An aliquot of the total cell lysate (HPE) was saved for Western blot analysis and the remaining sample was centrifuged (1,000 *xg*, 10 min, 4 °C) to remove nuclei and unbroken cells. The supernatant was centrifuged at 31,000 *xg* for 60 min to pellet crude plasma membranes (CPM).

2.6. Western Blot Analysis

Podocyte whole extracts (20 μg), membrane extracts (20 μg), recombinant human GST-tagged carbonic-anhydrase-II (rhCAII, 0.5 μg; Abnova, St. Taipei, Taiwan) were electrophoresed on 12% SDS-PAGE under reducing conditions and blotted on PVDF membrane (Bio-Rad Laboratories). The membranes were blocked with 0.1% TWEEN 20 and 0.5% powdered milk in PBS 1×. The reactivity of sera from patients with IgG4-related disease and healthy subjects (n = 6) against CAII was tested by blotting membranes with serum diluted 1:10 followed by mouse anti-human IgG4-HRP antibody (clone HP6025, 1:1,000; Life Technologies, Gaithersburg, MA). To confirm the specific reactivity of IgG4 against CAII, membranes were stripped and reprobed with a rabbit anti-human CAII antibody (1:10,000; Abcam) followed by a goat anti-rabbit IgG-HRP (1:5,000; Sigma-Aldrich) antibody. To assess the reactivity of sera from patients with IgG4-related disease against SOD2, recombinant human GST-tagged SOD2 (rSOD2, 0.6 μg, Abnova) was electrophoresed as above and membranes were blotted with serum diluted 1:10

followed by mouse anti-human IgG3-HRP antibody (1:1,000; Life Technologies). To screen the reactivity of IgG subclasses against SOD2 and CAII in patients' sera, recombinant human GST-tagged SOD2 (rSOD2, 0.6 μg, Abnova) and purified CAII (pCAII, 0.5 μg, Sigma-Aldrich) were electrophoresed as above and membranes were blotted with patient's serum diluted 1:10 followed by mouse anti-human IgG1-HRP antibody (clone HP6069, 1:1,000; Life Technologies), mouse anti-human IgG2-HRP antibody (clone HP6014, 1:500; Life Technologies), mouse anti-human IgG3-HRP antibody (clone HP6047, 1:500; Life Technologies) and mouse anti-human IgG4-HRP antibody (clone HP6025, 1:1,000; Life Technologies). Bands were visualized with the ECL Western blotting Detection Reagent (Pierce/Celbio, Pero, Italy).

2.7. Intracellular pH Determination

The method was previously described [9] and calibrated by using the following procedure. Podocytes were loaded with 8 μM BCECF-AM (Molecular Probes, Invitrogen) for 15 min in RPMI 1640 medium at 37 °C. The cells were washed and incubated for 10 min with a modified Ringer solution adjusted to different pH values (125 mM KCl, 1 mM $MgCl_2$, 1 mM $CaCl_2$, 20 mM Hepes) supplemented with nigericin (10 μM, Molecular Probes, Invitrogen). The fluorescence intensities were then determined at the cellular level by the multimode microplate reader TECAN Infinite M200® PRO (Tecan Group Ltd., Mannedorf, Schweiz) at an excitation wavelength of 490 nm and emission wavelength of 530 nm, and the values were used to generate a calibration curve. To evaluate changes in intracellular pH after podocyte stimulation, cells were incubated with 8 μM BCECF-AM in the last 15 min of the stimuli. The fluorescence intensity was determined as above and the intracellular pH was extrapolated from the calibration curve.

2.8. Mitochondrial Morphology and Membrane Potential Detection

The fluorescent probe MitoTracker® Red (Molecular Probes, Invitrogen), which covalently binds to mitochondrial proteins by reacting with free thiol groups of cysteine residues regardless of membrane potential, and JC-1 (Molecular Probes, Invitrogen), a mitochondrial membrane potential sensor, were used to monitor mitochondrial mass and membrane potential, respectively. The MitoTracker® (250 nM) or JC-1 (5 μg/ml) was added to podocytes in the last 30 min of the stimuli. Cells were then rinsed twice in cold PBS 1× and fixed. Nuclei were counterstained with DAPI. Samples were examined under confocal inverted laser microscopy (LSM 510 Meta).

2.9. Mitochondrial ROS Production

Mitochondrial ROS were measured using MitoSOX™ Red, a live-cell-permeant mitochondrial superoxide indicator (Molecular Probes, Invitrogen). Cells were exposed to 5 μM MitoSOX added to the medium for the final 30 min of the treatment. Cells were collected by trypsinization, washed and mitochondrial superoxide was determined by FACS (FACS Canto, BD Biosciences, MI, Italy). MitoSOX Red was excited by laser at 510 nm wavelength and data collected at 580 nm (FL2) channel. The data were expressed as mean intensity of MitoSOX fluorescence and % of MitoSOX fluorescent cells.

2.10. Cell Fixation and Embedding for Electron Microscopy

Cells seeded on Thermanox coverslips were fixed in 3.5% paraformaldehyde and 0.01% glutaraldehyde in 0.1 M phosphate buffer, pH 7.4, and then embedded in LR White resin (Electron Microscopy Sciences) according to the standard protocol. Briefly, cells were quickly dehydrated in a series of ethanol solutions (30, 40, 50, 60, 70%; 10 min each), and then incubated with a mix of 70% ethanol/resin (1:1) for 30 min, followed by pure resin. Samples were infiltrated overnight with a fresh portion of pure resin at 4 °C and then LR White resin was polymerized at 4 °C under UV light.

2.11. Immunogold Labeling

Fragments of kidney biopsies from the archives of the Nephrology Unit, Azienda Ospedaliera Papa Giovanni XXIII, Bergamo, Italy, were fixed in 3.5% paraformaldehyde and 0.01% glutaraldehyde in 0.1 M phosphate buffer, pH 7.4, dehydrated through ascending grades of alcohol and embedded in LRW resin (Electron Microscopy Sciences, EMS). Ultrathin sections (120 nm thick) were cut and mounted on 100-mesh copper grids. Antigen retrieval was performed in 10 mM citrate buffer, pH 6.0, and microwaved for 4–5 min. Non-specific labeling was blocked by 1% BSA in PBS and then sections were incubated with primary antibodies rabbit anti-human SOD2 (1:100; Millipore) and rabbit anti-human CAII (1:5,000, Abcam) followed by 12-nm gold conjugated goat anti-rabbit IgG (1:20; Jackson ImmunoResearch Laboratories). Sections were then contrasted with uranyl acetate. Ultrathin sections were examined and images were acquired using a Philips Morgagni transmission electron microscope (FEI Company, Eindhoven, The Netherlands).

2.12. Immunofluorescence Analysis on Renal Tissue

Kidney biopsy from our patient from the archives of Nephrology Unit, Azienda Ospedaliera Papa Giovanni XXIII, Bergamo, Italy, was snap-frozen in liquid nitrogen, embedded in OCT compound and used for immunofluorescence analysis. In addition, renal biopsies from an uninvolved portion of kidney collected from tumor nephrectomy specimens were obtained from 8 patients and used as controls. Written informed consent was obtained from all these patients. Sections (3 μm) were air-dried, fixed with cold acetone and washed with PBS. After blocking non-specific sites with 1% BSA, slides were incubated with rabbit anti-human SOD2 (1:50, Millipore), rabbit anti-human CAII (1:600, Abcam) and mouse anti-human podocalyxin (1:150, gift from Professor Robert Atkins, Department of Nephrology, Monash Medical Centre, Clayton, VIC, Australia) followed by the species-specific Cy3 or FITC-conjugated secondary antibodies (Jackson Immunoresearch Laboratories). IgG4 deposits were immunolocalized by FITC-conjugated anti-human IgG4 (1:50, Sigma-Aldrich). Nuclei were stained with DAPI. Negative controls were obtained by omitting primary antibodies from adjacent sections. Fluorescence was examined using an inverted confocal laser scanning microscope (LMS 510 Meta). Z-stack glomerular images were collected with a spacing of 0.37 μm. The co-localization areas were visualized in each confocal optical section within the Z-stack by using appropriate software (LSM 510 Meta).

2.13. Electron Microscopy Analysis of Mitochondria in Renal Biopsy

Renal biopsy samples were processed using the standard technique for transmission electron microscopy. Briefly, the fragments (1 mm^3) were fixed in 2.5% glutaraldehyde in 0.1 M cacodylate buffer (pH 7.4), postfixed in 1% osmium tetroxide, and dehydrated in alcohol for embedding in Epon resin. Ultrathin sections (100 nm) were cut on an EM UC7 ultramicrotome (Leica Microsystems, Mannheim, Germany), collected on copper grids, and stained with uranyl acetate and lead citrate for analysis.

2.14. Statistical Analysis

Results are expressed as mean ± SE. Data analysis was performed using the computer software Prism (GraphPad Software Inc., San Diego USA). Comparisons were made by analysis of variance (ANOVA) with Tukey post hoc test or unpaired or paired Student's T test as appropriate. Statistical significance was defined as $P < 0.05$.

2.15. Funding

The project was supported by a grant from the Halpin Foundation, Inc. (Jupiter, USA) and a contribution from Minetti S.p.a (Bergamo, Italy). These funding sources did not have any role in the manuscript.

3. Results

3.1. Patient parameters

Patient IgG4-RD1 is a 73-year-old male with a diagnosis of IgG4-related disease involving the lung and TIN. His laboratory parameters at time of sampling were: serum creatinine 0.79 mg/dl, protein excretion 77 mg/gCr, total IgG 3426 mg/dl and IgG4 1230 mg/dl.

Patient IgG4-RD2 is a 61-year-old male with a history of IgG4-related disease involving the lacrimal glands, salivary glands, and lung. In this patient a diagnosis of TIN was made. The patient suffered from a MALT-lymphoma and underwent surgery for a renal carcinoma. At time of sampling laboratory parameters were: serum creatinine 1.32 mg/dl, protein excretion 500 mg/gCr, total IgG 1876 mg/dl and IgG4 628 mg/dl.

Patient IgG4-RD3 is 54-year-old female with IgG4-related disease involving the lung, lymph nodes and aorta. She had autoimmune pancreatitis. The following values of laboratory parameters were found at the time of sampling: serum creatinine 0.71 mg/dl, protein excretion negative, total IgG 1968 mg/dl and IgG4 536 mg/dl.

Patient IgG4-RD4 is a 75-year-old male with IgG4-related disease involving the lacrimal glands and aorta. He suffered from autoimmune pancreatitis and is affected by TIN. His laboratory parameters at time of sampling were: serum creatinine 1.34 mg/dl, protein excretion 0.2 g/day, total IgG 5380 mg/dl and IgG4 587 mg/dl.

3.2. The Patient's IgG4 Specifically Recognizes Carbonic Anhydrase II on Cultured Podocytes

We found that IgG4 in our patient's serum recognized a recombinant GST-tagged CAII protein with a molecular weight of 55 kDa (Fig. 1A, first lane) as well as a 30 kDa protein corresponding to CAII in protein extracts from cultured human podocytes (Fig. 1A, second and third lanes, arrowhead). The possible existence of other unknown antigens could not be excluded because the patient's IgG4 also recognized other bands in the podocyte extracts (Fig. 1A, second lane). No IgG4 reactivity against CAII was found in sera from healthy subjects (Fig. 1A, right lane). Western blot analysis of purified CAII protein revealed that IgG4 was the predominant IgG subclass of anti-CAII antibodies in the patient's serum while reactivity of other IgG subclasses was absent (Fig. 1B). In podocytes, CAII clearly localized in the cytoplasm and at the cell periphery of permeabilized cells (Fig. 1C, left). We also found high CAII membrane expression in non-permeabilized cells (Fig. 1C, middle). CAII membrane localization was confirmed by the detection of a 30 kDa band using Western blotting in podocyte crude plasma membranes (Fig. 1C, right). Immunogold labeling confirmed CAII cytoplasmic and membrane expression in podocytes in a control subject's biopsy as shown in Fig. 1D.

3.3. Glomerular Expression of CAII in Healthy Controls and in IgG4-Related Disease Patient

Granular CAII was revealed in the glomeruli of control kidney biopsies (Fig. 2A) and was increased in the patient's sample, showing a granular pattern along the glomerular capillary walls (Fig. 2B). CAII was also expressed in tubuli of both control subjects, as previously reported [10] and the IgG4-related disease patient (Fig. 2A and B). Double immunostaining with CAII and the podocyte marker podocalyxin showed that CAII localized in podocytes (Fig. 2C). The co-localization was also confirmed in z-axis, as reported in Supplementary Fig. 1. In patient's glomeruli, double immunostaining documented that CAII strongly colocalized with deposited IgG4 (Fig. 2D). The co-localization between CAII and IgG4 was robust, albeit partial, and consistently present along the z-axis (Supplementary Fig. 2). Triple immunostaining revealed that CAII and IgG4 colocalized with podocalyxin (Fig. 2E). No IgG4 staining was found in renal biopsies of control subjects (Supplementary Fig. 3).

3.4. Patient's IgG4 Induces Cell Acidification, Mitochondrial Dysfunction and Cytoskeletal Remodeling in Podocytes

Based on the role of CAII in maintaining cellular pH [11], we asked whether the patient's IgG4 could interfere with intracellular pH control. We compared the effect of acetazolamide, a known CAII pharmacologic inhibitor, on intracellular pH with that of IgG4 immunopurified from the patient's serum. The intracellular pH time-dependently decreased in cultured podocytes after acetazolamide exposure (Fig. 3A). The patient's IgG4, but not the IgG4 isolated from healthy volunteers (control's IgG4), caused a pronounced drop in pH to very low levels, reproducing an even more powerful effect than that reached by the CAII inhibiting action of acetazolamide (Fig. 3A). Immunofluorescence analysis in cultured podocytes showed fragmentation of the mitochondrial network after exposure to the patient's IgG4, but not to the control's (Fig. 3B, left). This was associated with collapse of mitochondrial membrane potential (Fig. 3B, right) as revealed by a red-to-green shift of the fluorescence emission of the mitochondrial potential-sensitive probe. A similar effect on mitochondria was observed in podocytes exposed to hydrogen peroxide (H_2O_2) (Fig. 3B), known to generate reactive oxygen species (ROS), which mediate mitochondrial dysfunction. Electron microscopy analysis of the patient's renal biopsy showed mitochondrial alterations with matrix loss and cristae disorganization, which appears rather consistent with the *in vitro* findings. Those changes were variably associated with dense cytoskeletal-like cytoplasmic strands and junctional abnormalities (Fig. 3C). Podocyte exposure to either IgG4 from our patient or H_2O_2 triggered mitochondrial generation of superoxide anion as detected by the fluorescent dye MitoSOX at both 6 and 15 h (Fig. 3D and Supplementary Fig. 4). The patient's IgG4 induced only at 15 h a corticalization of F-actin filaments that, in contrast, were distributed across the cell body in the unstimulated or control's IgG4-treated podocytes (Fig. 3E). H_2O_2 also caused F-actin rearrangement to a lesser extent than the patient's IgG4 (Fig. 3E), suggesting a role for oxidative stress in cytoskeletal alteration. This was confirmed by the addition of the antioxidant MnTBAP, a mitochondrial-targeted SOD2-mimetic, which prevented F-actin corticalization in podocytes incubated with the patient's IgG4 (Fig. 3E).

3.5. Immunocompetent IgG4 Leads to SOD2 Mislocation on the Plasma Membrane Favoring Complement Deposition

Given that the antioxidant SOD2-mimetic reverted the effect of the patient's IgG4 on ROS-dependent cytoskeletal remodeling upon binding to CAII, and that SOD2 has previously been identified as a plasma membrane antigen for the IgG3 of this patient [4], we investigated the causal link between IgG4 anti-CAII and the mitochondrial SOD2 on the plasma membrane of injured podocytes. Exposure to the patient's IgG4 or H_2O_2 resulted in a significant increase in SOD2 staining on the podocyte surface (Fig. 4A and B). However, only the patient's IgG4 was able to elicit the SOD2 cluster formation on the podocyte membrane (Fig. 4A and C). The control's IgG4 had no effect (Fig. 4A–C). The patient's IgG4-induced SOD2 externalization was dependent on mitochondrial dysfunction, since Cyclosporin A – an inhibitory agent of the mitochondrial permeability transition pore [12] – significantly attenuated SOD2 expression on the podocyte surface (Supplementary Fig. 5). To further prove the functional link between anti-CAII antibody and SOD2 externalization, non-permeabilized cultured human podocytes were incubated with a specific anti-CAII antibody. After 15-hour incubation, a strong presence of SOD2 at the podocyte surface was observed (Fig. 4D, middle panel).

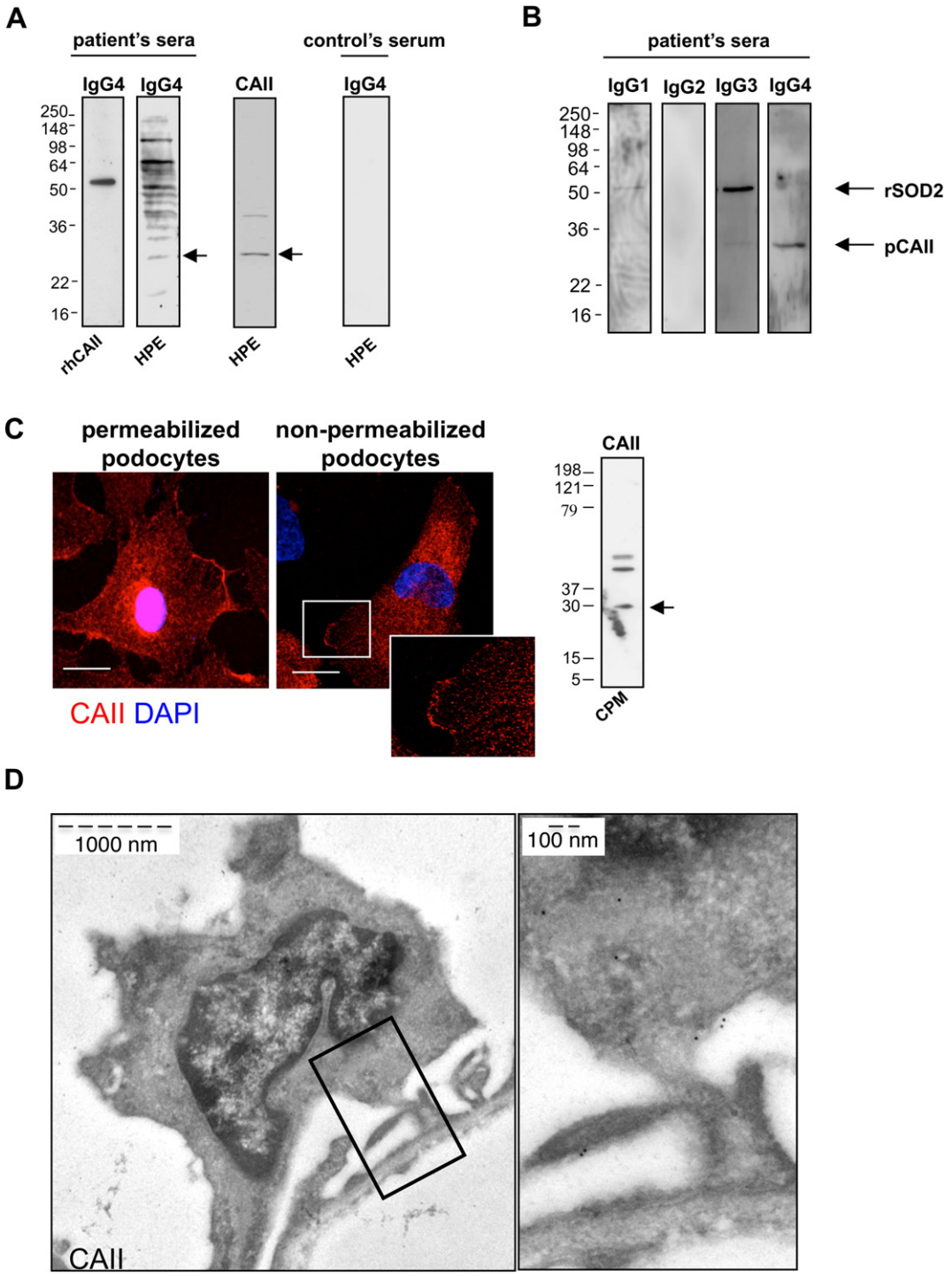

Fig. 1. Patient's IgG4 recognized CAII on podocytes. (A) Western blotting of the 55 kDa recombinant human GST-tagged CAII (rhCAII, 0.5 μg) or human podocyte extracts (HPE, 20 μg) with patient's (first and second lanes) or control's serum (fourth lane). IgG-subclass specificity was evaluated using an anti-human IgG4-HRP antibody. The HPE membrane was stripped and reprobed with a specific anti-human CAII antibody (third lane). Molecular weights (kDa) shown on the left side. (B) Western blotting of purified CAII (pCAII, 0.5 μg) and the recombinant human GST-tagged SOD2 (rSOD2, 0.6 μg) with patient's serum. IgG-subclass specificity was evaluated using an anti-human IgG1-HRP antibody, anti-human IgG2-HRP antibody, anti-human IgG3-HRP antibody or anti-human IgG4-HRP antibody. (C) CAII expression evaluated using immunofluorescence analysis (left) or Western blotting (right) of podocyte crude plasma membranes (CPM, 20 μg). Scale bars 20 μm. (D) CAII immunogold staining in normal human kidney.

SOD2 externalization was not detected when podocytes were exposed to normal IgG (Fig. 4D, right panel). In an additional set of experiments, cultured human podocytes were exposed to patient's serum either alone or following pre-exposure to purified CAII to specifically saturate the CAII binding sites of the patient's IgG4. The patient's serum alone elicited the formation of clustered SOD2 on the cell surface (Supplementary Fig. 6), effect that was not obtained when the patient's serum was previously pre-incubated with purified CAII (Supplementary Fig. 6).

To test the possibility that surface-exposed SOD2 could be recognized by anti-SOD2 IgG3 present in the patient's serum [4], we verified the co-localization of SOD2 and IgG3 on non-permeabilized podocytes. Similarly to the patient's IgG4, total IgG purified from the patient's

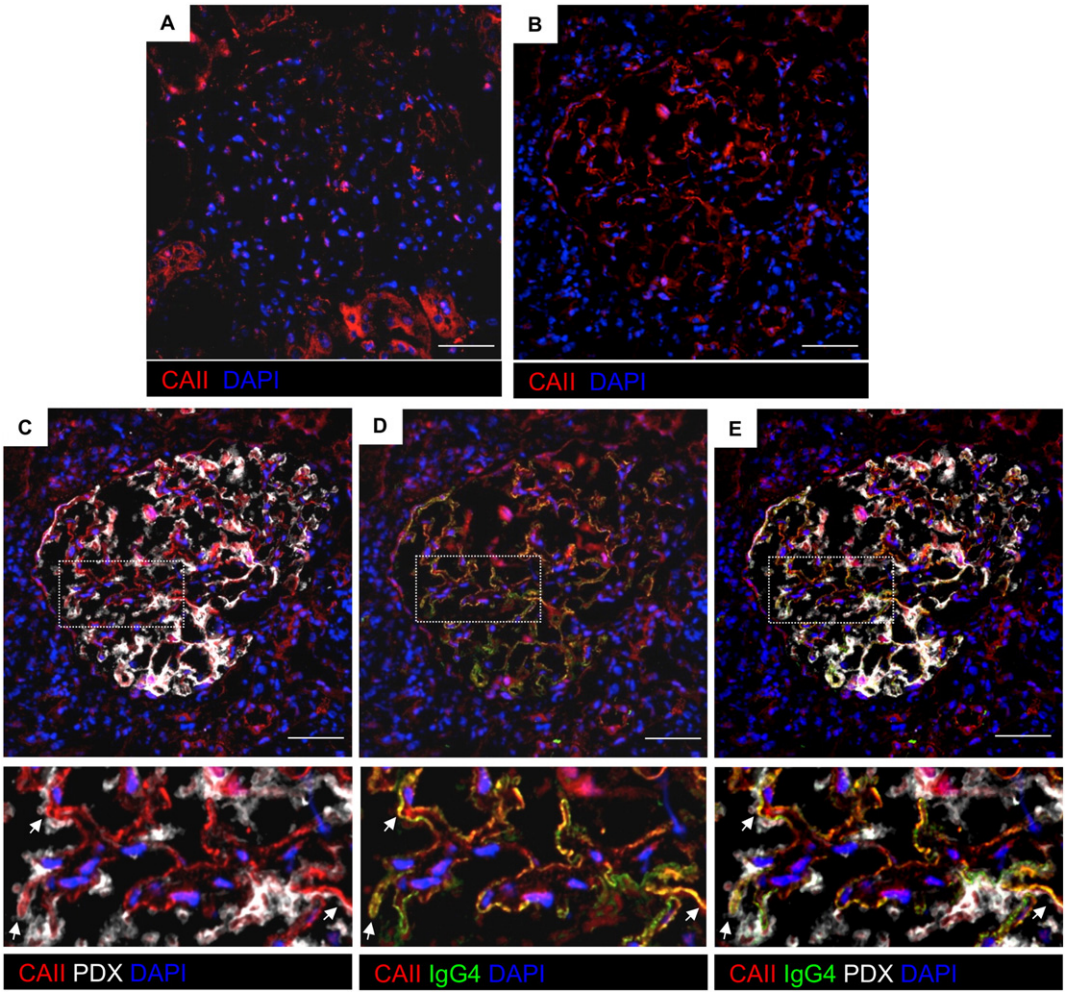

Fig. 2. Glomerular CAII increased and co-localized with IgG4 deposits in podocytes in patient's biopsy. (A and B) Representative images of CAII immunofluorescence in controls' (A) and patient's (B) glomeruli. (C) Co-localization between CAII (red) and PDX (white) in patient's sample. (D) Co-localization between CAII (red) and IgG4 (green) in patient's sample. (E) Triple immunostaining for CAII, IgG4 and PDX in patient's glomerulus. The details of the co-localization areas highlighted in insets are shown enlarged below, and indicated by arrows. Nuclei were stained with DAPI. Scale bars 50 μm.

serum promoted externalization of SOD2 that co-localized with IgG3 deposited with a granular distribution on podocyte membranes (Fig. 5A, upper panels). Immunoelectron microscopy of cultured podocytes confirmed that SOD2 was confined to the mitochondria of the control's IgG-treated podocytes while it was consistently found on the plasma membrane in cells exposed to the patient's IgG (Fig. 5A, lower panels). The patient's serum, as a source of complement and IgG, also induced complement activation and C3 recruitment to SOD2 (Fig. 5B). No effects were observed when the control's IgG or sera were used (Fig. 5A and B). To further assess the potential role of the SOD2/anti-SOD2 system in the MN pattern found in our patient, we determined the glomerular localization of SOD2 in biopsy tissue. SOD2 was not detectable in normal kidney glomeruli. We found granular peripheral SOD2 staining along the patient's glomerular capillary walls (Fig. 5C). This staining in MN reflected extracellular localization and accumulation of both antigen and anti-SOD2 antibodies in subepithelial deposits [5]. We found an identical granular pattern for IgG3, which is the predominant subtype within our patient's deposits. Notably, IgG3 is the anti-SOD2 IgG subtype detected in the patient's blood [4].

To verify the potential pathogenic role of the IgG4-dependent intracellular mechanisms identified, we extended our observations to other IgG4-related disease patients. In a set of four untreated IgG4-related disease patients, we identified three sera containing IgG4 anti-CAII and one negative for these autoantibodies (Fig. 6A). Similarly to our propositus' serum, only CAII-positive sera were able to elicit a drop in intracellular pH (Fig. 6B), markedly externalize SOD2 (Fig. 6C, left panel), and cluster it on the podocyte membrane (Fig. 6C, right panel). Despite the effect of autoreactive IgG4 anti-CAII on SOD2 expression in podocytes, we detected no IgG3 anti-SOD2 in any tested sera (Fig. 6D).

4. Discussion

The majority of patients with IgG4-related disease, particularly when associated with autoimmune pancreatitis, have circulating IgG4 subclass antibodies that recognize CAII [13,14]. The patient with hyper-IgG4 described here does indeed have both circulating IgG4 reacting with CAII and MN, and we disclose a functional link between the binding of the patient's IgG4 to podocytes and the intracellular events underlying the development of the MN lesion. CAII is expressed in most segments of the human kidney, including proximal and distal tubules [10]. In addition to its typical cytosolic distribution, CAII has been found to localize close to the plasma membrane where it interacts with the electroneutral Cl^-/HCO_3^- anion exchanger 1, giving rise to a transport metabolon wherein HCO_3^- is transferred from CAII to the anion exchanger, maximizing its cotransporter activity [15].

Here we found that podocytes, both *in vitro* and in kidney-biopsy tissue sections, express CAII. Furthermore, IgG4 purified from the patient's serum elicits early intracellular acidification with profound effects on podocyte homeostasis as a likely consequence of the interaction of IgG4

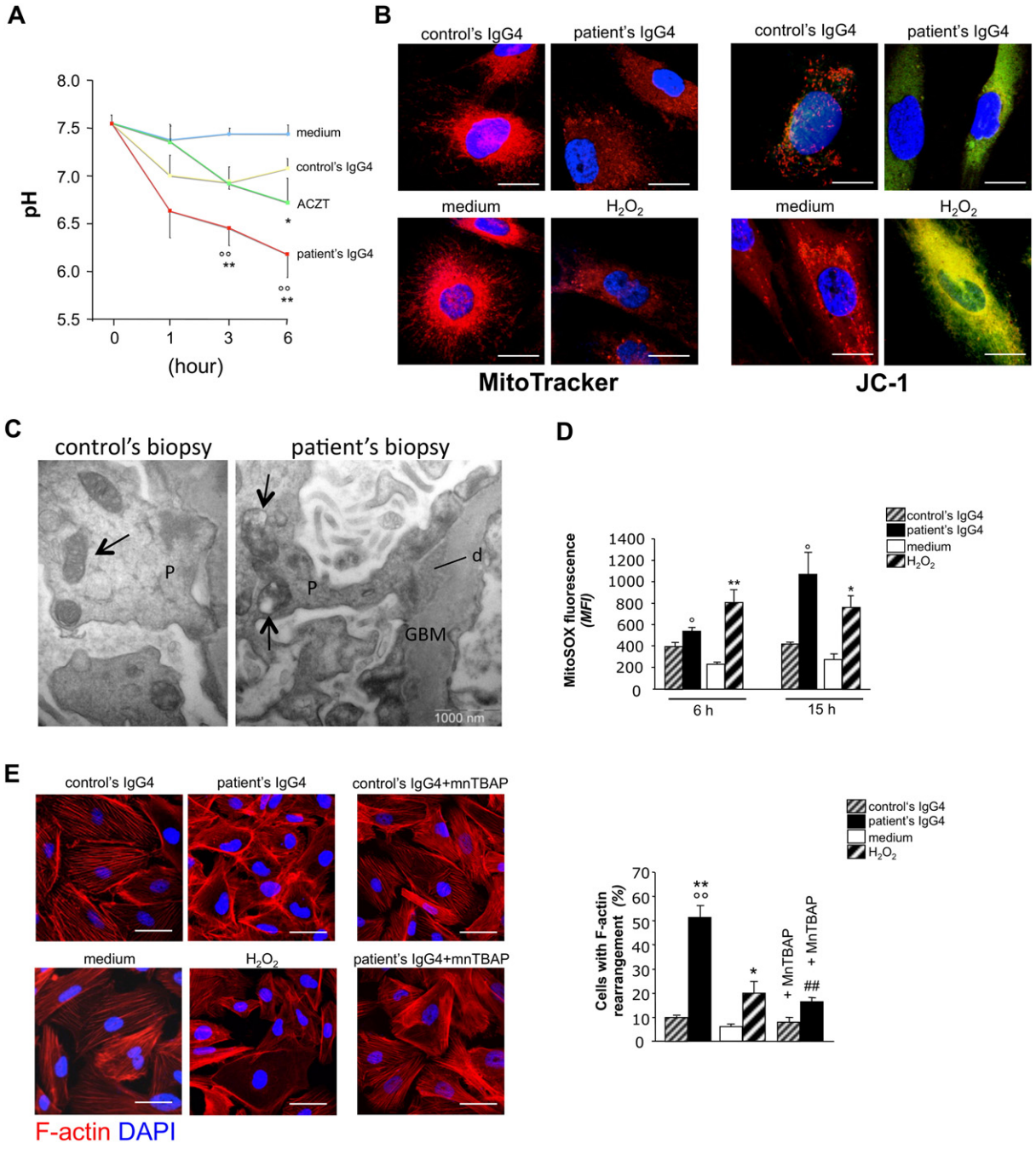

Fig. 3. Cell acidification, mitochondrial alterations and ROS-dependent cytoskeletal dysfunction induced by patient's IgG4. (A) Fluorimetric assay detecting intracellular pH in podocytes exposed to control's or patient's IgG4 (100 μg/ml), control medium (medium) or acetazolamide (ACZT, 500 nM). °°$p < 0.01$ vs control's IgG4; *$p < 0.05$, **$p < 0.01$ vs medium ($n = 4$ experiments). (B) Representative images of mitochondria labeled with MitoTracker (left panel) or the mitochondrial membrane potential sensor JC-1 (right panel) in podocytes exposed 6 h to control's or patient's IgG4 (100 μg/ml), control medium (medium) or H_2O_2 (150 μM). JC-1 accumulates in intact mitochondria resulting in a red emission, while it presents diffuse cytosolic green fluorescence in cells with depolarized mitochondria. Nuclei were stained with DAPI (blue). Scale bars 20 μm. (C) Electron micrographs of mitochondria (arrows) in podocyte from control's and our propositus' biopsy, showing reduced density of matrix and loss of cristae. P, podocyte; GBM, glomerular basement membrane; d, subepithelial electron-dense deposit. (D) Mitochondrial oxidative stress assessed as $O_2^{\bullet -}$ generation using MitoSOX flow cytometry measuring mean fluorescence intensity (MFI). Results are mean ± SE. °$p < 0.05$, °°$p < 0.01$ vs control's IgG4; *$p < 0.05$, **$p < 0.01$ vs medium ($n = 3$ experiments). (E) Representative images and quantification of F-actin (red) rearrangement in podocytes exposed 15 h to control's or patient's IgG4 (100 μg/ml), control medium (medium), or H_2O_2 (150 μM). Nuclei were stained with DAPI (blue). Scale bars 50 μm. In additional experiments, MnTBAP (100 μM) was used. Results (mean ± SE) are expressed as percentage of cells with F-actin rearrangement. °°$p < 0.01$ vs control's IgG4; *$p < 0.05$ vs medium; ##$p < 0.01$ vs patient's IgG4 ($n = 4$ experiments).

autoantibodies with membrane CAII. The drop in cytosolic pH over time is even greater than the acidification elicited by a specific pharmacologic CAII inhibitor, indicating direct and potent inhibitory action of the patient's IgG4 on podocyte CAII that can behave as a functional pathogenic target. Notably, this interaction is reminiscent of the ability of non-complement-fixing IgG4 autoantibodies to interact with an antigen in terms of inhibiting its function, as has been shown for IgG4 to muscle-specific kinase in patients with myasthenia gravis [16,17] and suggested for anti-PLA_2R antibodies in patients with idiopathic MN [18,19]. In this regard, in the case of our patient, the co-localization of CAII

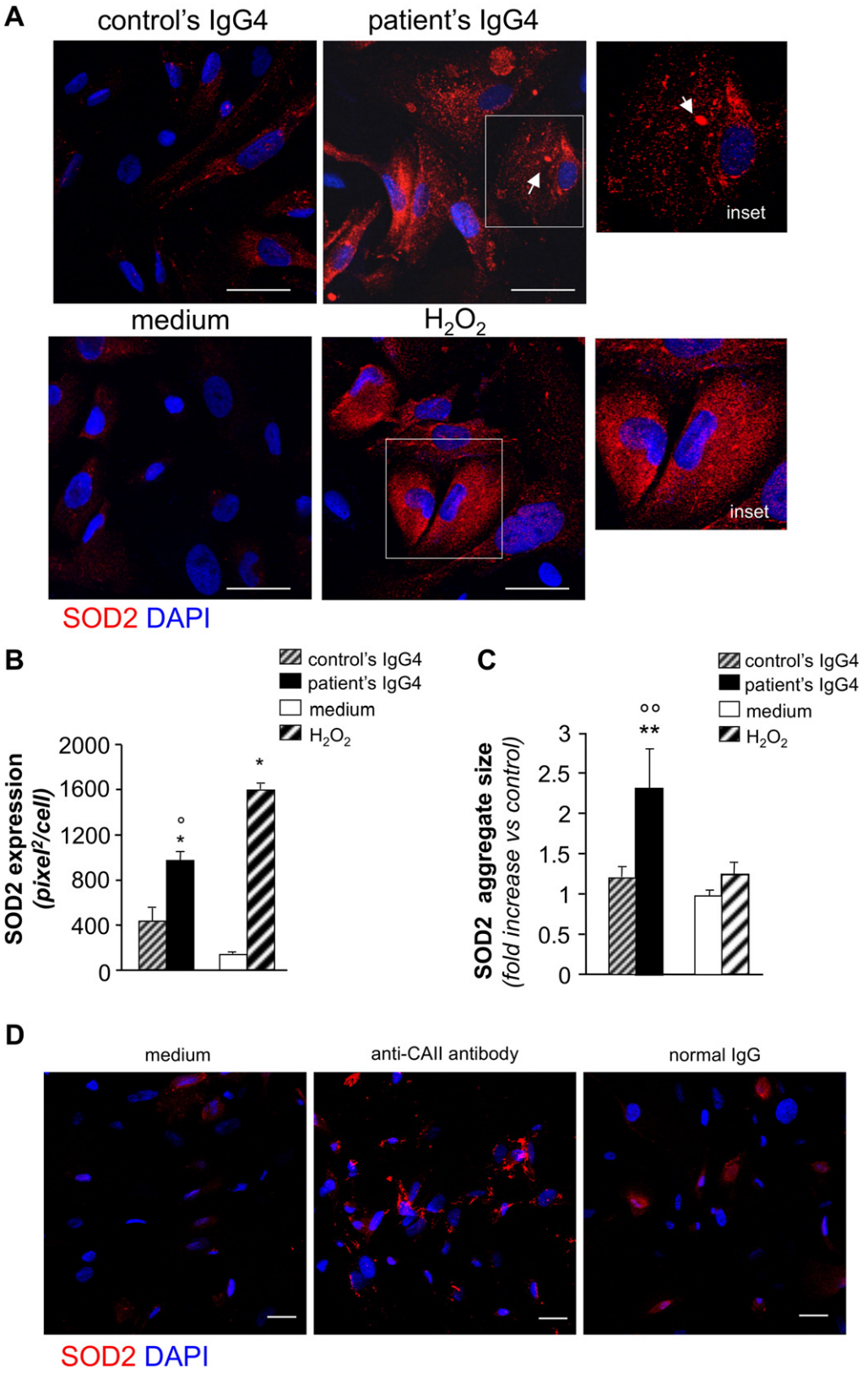

Fig. 4. Patient's IgG4 leads to SOD2 externalization to podocyte plasma membrane. (A) Representative images of SOD2 expression (red) on the surface of cultured human podocytes exposed 15 h to control's or patient's IgG4 (100 μg/ml), control medium (medium) or H_2O_2 (150 μM). Clustered SOD2 is indicated with arrowhead. Nuclei were stained with DAPI (blue). Scale bars 50 μm. (B, C) Histograms show quantification of surface staining (B) and mean average size (C) of SOD2 clusters on podocyte plasma membrane expressed as mean ± SE. °$p < 0.01$ vs control's serum; *$p < 0.01$ vs medium ($n = 8$ experiments). (D) Representative images of SOD2 expression (red) on the surface of cultured human podocytes exposed for 15 h to control medium (medium), commercially available anti-CAII antibody (5 μg/ml), or normal IgG (5 μg/ml). Nuclei were stained with DAPI (blue). Scale bars 50 μm. ($n = 3$ experiments).

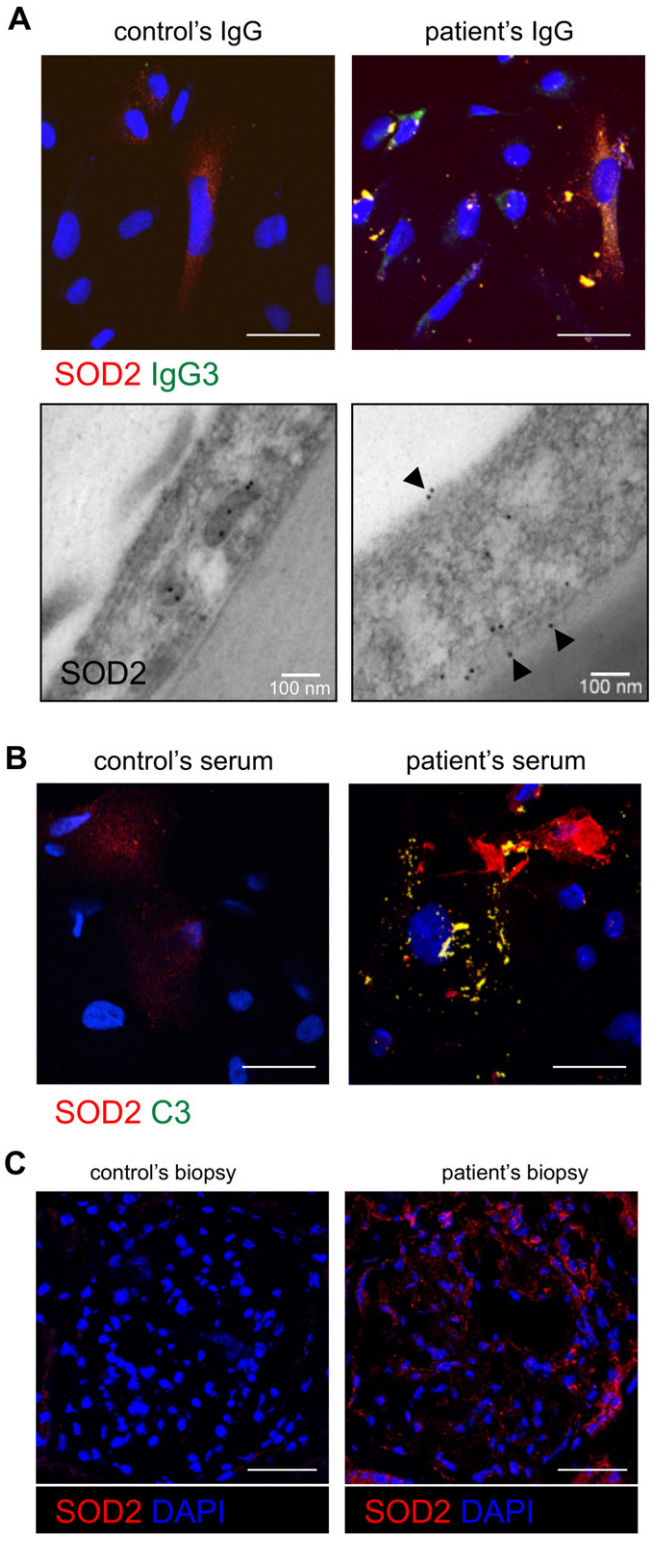

Fig. 5. Patient's IgG3, by binding externalized SOD2, favored complement activation. (A, upper panel) Co-localization (yellow) of SOD2 (red) and IgG3 (green) on non-permeabilized podocytes exposed to total IgG fraction (1 mg/ml) immunopurified from control's or patient's serum. Nuclei were stained with DAPI (blue). Scale bars 50 μm. (A, lower panel) Representative electron micrographs of immunogold labeling of SOD2 in podocytes exposed to control's or patient's total IgG fraction. Gold particles localized on the plasma membrane in patient's IgG-treated cells (arrowheads). (B) Co-localization (yellow) of SOD2 (red) and complement C3 (green) on non-permeabilized podocytes exposed to control's or patient's serum. Nuclei were stained with DAPI (blue). Scale bars 50 μm. (C) Immunofluorescence analysis of SOD2 (red) renal expression in control's and in our IgG4-related disease patient's biopsy. Nuclei were stained with DAPI (blue). Scale bars 50 μm.

and IgG4 deposited in the glomeruli indicates that CAII is indeed present in the subepithelial immune deposits. This observation offers an important clue, which suggests that anti-CAII antibodies, which in our patient are restricted to the IgG4 subtype, could be responsible for initiating the disease.

Relying on evidence of mitochondrial disruption after early acidification in response to injurious stimuli [20], we next analyzed the consequences of low pH on mitochondrial functions. Our data that the decrease of podocyte pH preceded mitochondrial alteration and fragmentation provide a link between IgG4-driven intracellular acidification and perturbation of mitochondrial dynamics. Mitochondrial dysfunction in IgG4-treated podocytes was associated with massive ROS production, which in turn promoted F-actin cytoskeletal alterations. In this regard, an important role for ROS in inducing cytoskeletal reorganization in injured podocytes has been documented [21].

Another major finding of the study consists in the externalization of the mitochondrial enzyme SOD2 in clusters in direct response to the patient's IgG4-CAII ligation *in vitro*. The causal role of IgG4 anti-CAII challenge on SOD2 externalization is provided by the combined evidence that incubating the cells with an anti-CAII antibody induced the mislocation of SOD2 on the podocyte surface and that the saturation of patient's serum antibodies with purified CAII prevented the SOD2 mobilization. This would indicate a direct effect of the patient's IgG4 anti-CAII in the activation of intracellular signaling that leads to SOD2 trafficking to the podocyte plasma membrane. The observed mitochondrial fragmentation along with the consequent altered membrane potential in response to anti-CAII IgG4 could affect the release of matrix proteins from failing mitochondria [22], including SOD2. The finding that prevention of mitochondrial depolarization attenuated IgG4-induced SOD2 externalization on the membrane of damaged podocytes points to mitochondrial dysfunction as the major cause of SOD2 mislocation after exposure to the patient's IgG4.

Protein membrane trafficking in podocytes is regulated by cytoskeletal F-actin filaments [23] and cytoskeletal alterations have been associated with SOD2 mistargeting from spoiled mitochondria to the cell surface [24]. Here we suggest that the patient's IgG4-induced cytoskeletal F-actin corticalization could drag the released SOD2 toward the plasma membrane and influence its spatial patterning in podocytes. In line with our findings, a local enrichment of cortical actin filaments was found to regulate nanocluster formation of membrane proteins [25]. The role of cytoskeletal remodeling in SOD2 cluster formation rests on the evidence that H_2O_2, while promoting strong SOD2 externalization, did not induce the SOD2 cluster formation. This difference could conceivably be a consequence of the lower capacity of H_2O_2 to induce F-actin corticalization compared to IgG4. The consequent C3 deposition on the cell surface indicates that the externalized SOD2 is the target for the binding of the patient's IgG3, leading to complement activation. Since SOD2 becomes recognizable on the podocyte surface via a process that can be related to the patient's IgG4 and is induced with disease, SOD2 behaves like a neoantigen, as other intracellular proteins, which are not abundantly expressed in the normal glomerulus [19]. Given the absence of detectable circulating immune complexes in our patient and according to known disease models, these findings converged to suggest intraglomerular interaction between IgG3 and SOD2 further shaping the MN lesion in the presence of anti-CAII IgG4 (see scheme Fig. 6E).

Although SOD2 has been suggested as a possible neoantigen in non-PLA_2R associated MN, it is not clear whether or not the anti-SOD2 antibodies could worsen the existing disease or be informative as to its immunologic duration [19]. Together, our data lend further support to the view that SOD2 is not a primary antigen in MN, and in our patient. On the other hand, the early nature of anti-CAII IgG4-dependent podocyte injury could be suggested by findings that among additional patients with IgG4-related disease, only the sera of those with IgG4 anti-CAII antibodies promoted *in vitro* externalization and clustering of SOD2. The fact that not all of them could develop full-blown MN can be explained by multiple factors that possibly include genetic risks,

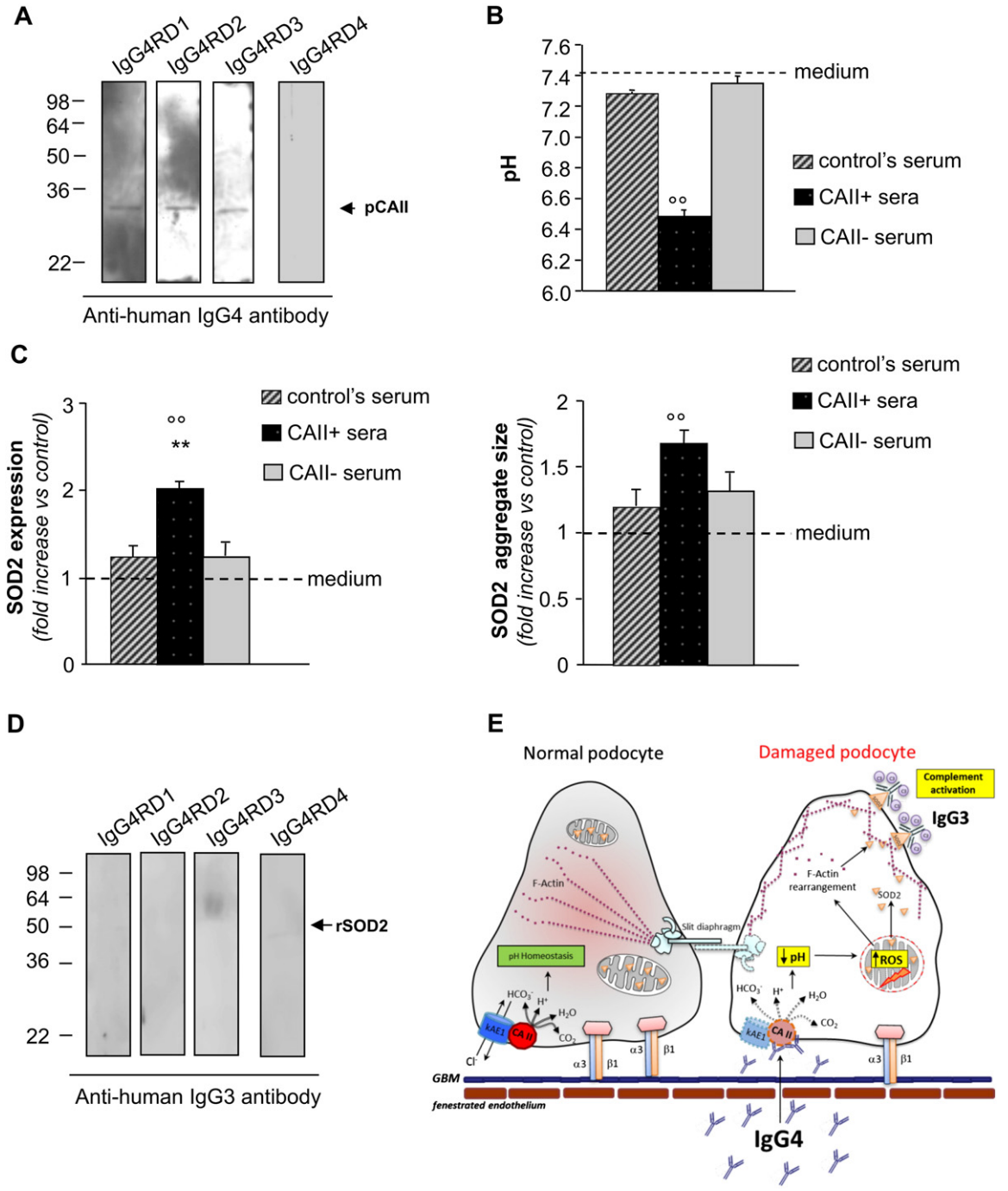

Fig. 6. Effect of IgG4 anti-CAII in sera of untreated IgG4-related disease patients. (A) Western blotting of purified CAII (pCAII, 0.6 μg). IgG-subclass specificity against CAII was evaluated using an anti-human IgG4-HRP antibody. (B) Intracellular pH detected using fluorimetric assay in podocytes exposed 6 h to IgG4 anti-CAII positive sera (CAII + sera), IgG4 anti-CAII negative serum (CAII − sera), control's serum (control's serum) or control medium (medium). °°$p < 0.01$ vs control's IgG4; *$p < 0.05$, **$p < 0.01$ vs medium ($n = 4$ experiments). (C) Histograms show the quantification of surface staining (left) and the mean average size of the SOD2 clusters (right) expressed as mean ± SE. °$p < 0.01$ vs control's serum; *$p < 0.01$ vs medium ($n = 8$ experiments). (D) Western blotting of recombinant SOD2 (rSOD2, 0.6 μg). IgG-subclass specificity against SOD2 was evaluated using an anti-human IgG3-HRP antibody. (E) Schematic representation of the proposed mechanism by which IgG4 promotes podocyte dysfunction, SOD2 externalization on the plasma membrane and C3-fixing IgG3 deposition. CAII, carbonic-anhydrase-II; C3, complement component 3; GBM, glomerular basement membrane; kAE1, kidney anion exchanger 1; ROS, reactive oxygen species.

epitope spreading, preformed or natural IgG against SOD2, duration, or insults such as a microbial infection as suggested for PLA_2R-associated MN [19]. Duration in particular might be important both in primary and secondary forms of the disease. In patients with autoimmune pathologies like systemic lupus erythematosus, a series of autoimmune changes leads to the appearance of different autoantibodies that usually precede the onset of clinical illness by many years [26]. Remarkably in this context, in all IgG4-related disease patients described to date, CAII antibodies were mutually exclusive with PLA2R antibodies, like the recently recognized Thrombospondin Type-1 Domain-Containing 7A antibodies do in idiopathic MN patients [27], which would be entirely consistent with CAII as a primary target in podocytes at least in our patient.

Advances in identifying novel biomarkers, including serological signatures and early key autoantibodies, provide a predictable tool for diagnosing and screening for disease while patients are still asymptomatic. Likewise, the identification of autoantibodies involved in early-stage MN pathogenesis, possibly including IgG4 anti-CAII antibodies in a subset of patients, may provide a crucial site for potential therapeutic

intervention to halt the initial MN lesions and the ensuing clinical onset of the pathology.

Supplementary data to this article can be found online at http://dx.doi.org/10.1016/j.ebiom.2015.03.003.

Conflicts of Interest

All the authors declare no conflicts of interest.

Author Contributions

S.B. and L.P. carried out in vitro studies and contributed equally to the study design, data analysis and interpretation, and writing the manuscript; M.G. carried out western blot analyses, IgG isolation, collected and assembled data, analyzed and interpreted data, wrote the manuscript; M.A. carried out electron microscopy studies, collected and assembled data, analyzed and interpreted data, wrote the manuscript; M.M. conceived and designed the experiments, analyzed and interpreted data, wrote the manuscript; R.N. carried out immunohistochemistry experiments on biopsies; E.G. conceived and designed the experiments, collected and assembled data, analyzed and interpreted data, wrote the manuscript; C.T. carried out western blot analyses and IgG isolation; D.R. carried out electron microscopy studies; E.S. provided renal biopsy and plasma samples of the propositus; T. Saito contributed to editing the manuscript; M.K. and T. Saeki provided sera from patients with IgG4-related disease; C.Z. interpreted data and edited the manuscript; G.R. and A.B. contributed equally in the data interpretation, in the writing of the manuscript and approval of the final version.

Acknowledgments

We are greatly indebted to Prof. Michael Goligorsky for the constructive criticisms and suggestions during the “Scientific Writing Academy” held at Mario Negri Institute in Ranica, Bergamo, Italy. We thank Debora Conti for preparing cell cultures and Daniela Cavallotti for biopsy sample processing. Manuela Passera and Kerstin Mierke helped to prepare and edit the manuscript. Luca Perico is recipient of a fellowship from “Fondazione Aiuti per la Ricerca sulle Malattie Rare (ARMR)”, Bergamo, Italy.

References

[1] Stone, J.H., Zen, Y., Deshpande, V., 2012]. IgG4-related disease. N. Engl. J. Med. 366, 539–551.
[2] Saeki, T., Nishi, S., Imai, N., et al., 2010]. Clinicopathological characteristics of patients with IgG4-related tubulointerstitial nephritis. Kidney Int. 78, 1016–1023.
[3] Alexander, M.P., Larsen, C.P., Gibson, I.W., et al., 2013]. Membranous glomerulonephritis is a manifestation of IgG4-related disease. Kidney Int. 83, 455–462.
[4] Cravedi, P., Abbate, M., Gagliardini, E., et al., 2011]. Membranous nephropathy associated with IgG4-related disease. Am. J. Kidney Dis. 58, 272–275.
[5] Prunotto, M., Carnevali, M.L., Candiano, G., et al., 2010]. Autoimmunity in membranous nephropathy targets aldose reductase and SOD2. J. Am. Soc. Nephrol. 21, 507–519.
[6] Hjelm, H., Hjelm, K., Sjoquist, J., 1972]. Protein a from *Staphylococcus aureus*. Its isolation by affinity chromatography and its use as an immunosorbent for isolation of immunoglobulins. FEBS Lett. 28, 73–76.
[7] Gagliardini, E., Perico, N., Rizzo, P., et al., 2013]. Angiotensin II contributes to diabetic renal dysfunction in rodents and humans via Notch1/Snail pathway. Am. J. Pathol. 183, 119–130.
[8] Mitsumoto, Y., Klip, A., 1992]. Development regulation of the subcellular distribution and glycosylation of GLUT1 and GLUT4 glucose transporters during myogenesis of l6 muscle cells. J. Biol. Chem. 267, 4957–4962.
[9] James-Kracke, M.R., 1992]. Quick and accurate method to convert BCECF fluorescence to pHi: calibration in three different types of cell preparations. J. Cell. Physiol. 151, 596–603.
[10] Purkerson, J.M., Schwartz, G.J., 2007]. The role of carbonic anhydrases in renal physiology. Kidney Int. 71, 103–115.
[11] Boron, W.F., 2010]. Evaluating the role of carbonic anhydrases in the transport of HCO3-related species. Biochim. Biophys. Acta 1804, 410–421.
[12] Heusch, G., Boengler, K., Schulz, R., 2010]. Inhibition of mitochondrial permeability transition pore opening: the Holy Grail of cardioprotection. Basic Res. Cardiol. 105, 151–154.
[13] Aparisi, L., Farre, A., Gomez-Cambronero, L., et al., 2005]. Antibodies to carbonic anhydrase and IgG4 levels in idiopathic chronic pancreatitis: relevance for diagnosis of autoimmune pancreatitis. Gut 54, 703–709.
[14] Pertovaara, M., Bootorabi, F., Kuuslahti, M., Pasternack, A., Parkkila, S., 2011]. Novel carbonic anhydrase autoantibodies and renal manifestations in patients with primary Sjogren's syndrome. Rheumatology (Oxford) 50, 1453–1457.
[15] Sowah, D., Casey, J.R., 2011]. An intramolecular transport metabolon: fusion of carbonic anhydrase II to the COOH terminus of the Cl(−)/HCO(3)(−)exchanger, AE1. Am. J. Physiol. Cell Physiol. 301, C336–C346.
[16] Klooster, R., Plomp, J.J., Huijbers, M.G., et al., 2012]. Muscle-specific kinase myasthenia gravis IgG4 autoantibodies cause severe neuromuscular junction dysfunction in mice. Brain 135, 1081–1101.
[17] Huijbers, M.G., Zhang, W., Klooster, R., et al., 2013]. MuSK IgG4 autoantibodies cause myasthenia gravis by inhibiting binding between MuSK and Lrp4. Proc. Natl. Acad. Sci. U. S. A. 110, 20783–20788.
[18] Beck Jr., L.H., Bonegio, R.G., Lambeau, G., et al., 2009]. M-type phospholipase A2 receptor as target antigen in idiopathic membranous nephropathy. N. Engl. J. Med. 361, 11–21.
[19] Beck Jr., L.H., Salant, D.J., 2014]. Membranous nephropathy: from models to man. J. Clin. Invest. 124, 2307–2314.
[20] Matsuyama, S., Reed, J.C., 2000]. Mitochondria-dependent apoptosis and cellular pH regulation. Cell Death Differ. 7, 1155–1165.
[21] Hsu, H.H., Hoffmann, S., Endlich, N., et al., 2008]. Mechanisms of angiotensin II signaling on cytoskeleton of podocytes. J. Mol. Med. 86, 1379–1394.
[22] Igbavboa, U., Zwizinski, C.W., Pfeiffer, D.R., 1989]. Release of mitochondrial matrix proteins through a Ca2+-requiring, cyclosporin-sensitive pathway. Biochem. Biophys. Res. Commun. 161, 619–625.
[23] Arif, E., Wagner, M.C., Johnstone, D.B., et al., 2011]. Motor protein Myo1c is a podocyte protein that facilitates the transport of slit diaphragm protein Neph1 to the podocyte membrane. Mol. Cell. Biol. 31, 2134–2150.
[24] Sinclair, L., Lewis, V., Collins, S.J., Haigh, C.L., 2013]. Cytosolic caspases mediate mislocalised SOD2 depletion in an in vitro model of chronic prion infection. Dis. Model Mech. 6, 952–963.
[25] Gowrishankar, K., Ghosh, S., Saha, S., C.R., Mayor, S., Rao, M., 2012]. Active remodeling of cortical actin regulates spatiotemporal organization of cell surface molecules. Cell 149, 1353–1367.
[26] Arbuckle, M.R., McClain, M.T., Rubertone, M.V., et al., 2003]. Development of autoantibodies before the clinical onset of systemic lupus erythematosus. N. Engl. J. Med. 349, 1526–1533.
[27] Tomas, N.M., Beck Jr., L.H., Meyer-Schwesinger, C., et al., 2014]. Thrombospondin type-1 domain-containing 7A in idiopathic membranous nephropathy. N. Engl. J. Med. 371, 2277–2287.